Probing the Mechanism of CO2 Capture in Diamine-Appended Metal-Organic Frameworks Using Measured and Simulated X-ray Spectroscopy

Supporting Information

Walter S. Drisdell[1], Roberta Poloni[2], Thomas M. McDonald[3], Tod A. Pascal[4], Liwen F. Wan[4], C. Das Pemmaraju[4], Bess Vlaisavljevich[5], Samuel O. Odoh[6], Jeffrey B. Neaton[4], Jeffrey R. Long[1,3], David Prendergast[4], Jeffrey B. Kortright[1*]

*[1]Materials Sciences Division, Lawrence Berkeley National Laboratory, Berkeley, CA 94720, USA. [2]Université Grenoble Alpes, Science et Ingénierie des Matériaux et Procédés (SIMAP), F-38000 Grenoble, France. [3]Department of Chemistry, University of California, Berkeley, California 94720, USA. [4]Molecular Foundry, Lawrence Berkeley National Laboratory, Berkeley, California 94720, USA. [5]Department of Chemical and Biological Engineering, University of California, Berkeley, California 94720, USA. [6]Department of Chemistry, Chemical Theory Center and Supercomputing Institute, University of Minnesota, Minneapolis, Minnesota 55455, USA. *Corresponding Author.*

1 Supplemental DFT Calculations

1.1 Density of States Calculations

In order to ascertain the relative energy positions of occupied and empty molecular orbitals with significant carbamate oxygen 2*p* character we calculated the projected density of states (PDOS) for the ground-state electronic configuration of the insertion and chain structures. The

PDOS was calculated using the same planewave ultrasoft pseudopotential framework within the Quantum Espresso[1] package that was employed for simulating the NEXAFS spectra.

1.2 Full Core Hole (FCH) Calculations

To further investigate whether the observed differences in the carbamate O 1*s* → π* NEXAFS transition energies between the insertion and chain structures arises primarily from differences in the empty π* orbitals or O 1*s* core orbitals, we estimated relative O 1*s* core-level binding energies on various O sites in the two structures. This is achieved by calculating the relative O 1*s* core-ionization energies using the *Full Core Hole* (FCH) approach.[2] Within this approach, the core-ionized atom is modeled using a core-hole pseudopotential just as in the case of the NEXAFS simulations but the core-electron is considered to be removed to infinity. The core-level binding energy difference ΔE_{CL} between two atoms of the same element *X* in two different chemical systems *A* and *B* (or equivalently two different chemical environments within the same system) is given by

$$\Delta E_{CL} = \{(E^{FCH}_{X,A} - E^{GS}_{A}) - (E^{FCH}_{X,B} - E^{GS}_{B})\}$$

where $E^{FCH}_{X,A}$, $E^{FCH}_{X,B}$ represent total energies of the simulation cell when a given atom of element X in systems A and B respectively is core-ionized and E^{GS}_{A},E^{GS}_{B} represent corresponding ground state energies of the two systems. The FCH energies and core-level shifts were calculated using the same numerical parameters employed in the NEXAFS simulaitons.

1.3 PDOS and FCH Analysis

The computed PDOS for the insertion and chain structures is shown in Figure S5. The splitting between the occupied and empty states for the carbamate O atoms is roughly the same

in each case (~5.682 eV for the insertion structure and ~5.516 eV for the chain structure). This implies that the higher energy π* resonance for the carbamate O atoms in the insertion structure is not due to a larger π- π* splitting. The computed FCH energies, however, reveal a distinct difference between the two structures. FCH energies were computed for representative carbamate O atoms for each structure as well as the three different O atoms on the organic linker ligand in each structure (two carboxylate O atoms and one hydroxyl oxygen). For comparison, the hydroxyl FCH energy is set to zero for each structure, under the assumption that the linker will be largely unaffected by CO_2 adsorption in both cases.

The results show that the carbamate O atoms in the insertion structure have significantly deeper core levels than those in the chain structure (1.27 eV and 0.71 eV deeper). The deepest core level corresponds to the oxygen that is directly bonding with the Mg in the insertion structure, consistent with a withdrawal of electron density due to this bond. Therefore the higher energy π* resonance for this structure when compared with the chain structure is a signature of insertion, arising from a screening effect due to the direct interaction with the Mg site.

Table S1

Insertion Structure		Chain Structure	
Oxygen	**FCH energy (eV)**	**Oxygen**	**FCH energy (eV)**
Linker Hydroxyl	0	Linker Hydroxyl	0
Linker carboxylate trans	0.3342589949	Linker carboxylate trans	0.423639985
Linker carboxylate cis	0.4690222669	Linker carboxylate cis	0.2347997805
Carbamate-Mg	0.4227530229	Carbamate-free	-0.8440626064
Carbamate-free	0.4192669448	Carbamate-N	-0.2909815302

Linker:

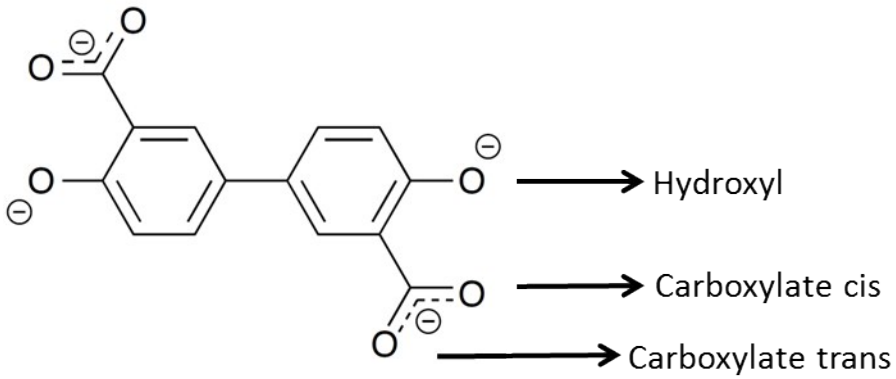

Insertion Structure:

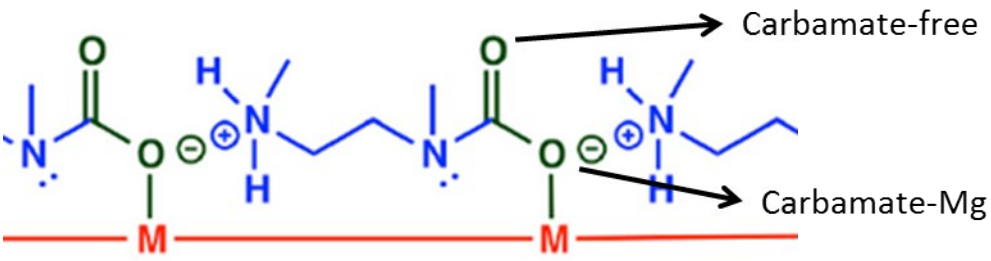

Chain Structure:

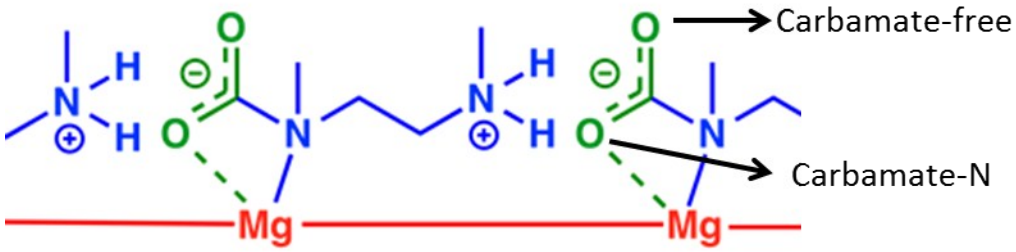
Carbamate-free
Carbamate-N
O
H
N
H
O
N
H
O
Mg
Mg

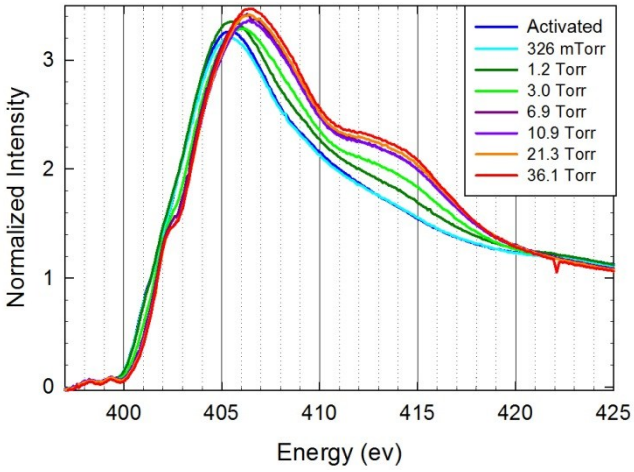

Figure S1: Experimental N K-edge spectra of mmen-Mg_2(dobpdc) in vacuum and under increasing pressures of CO_2 gas. Spectral changes are first visible at 1.2 Torr, and the system is saturated by 6.9 Torr.

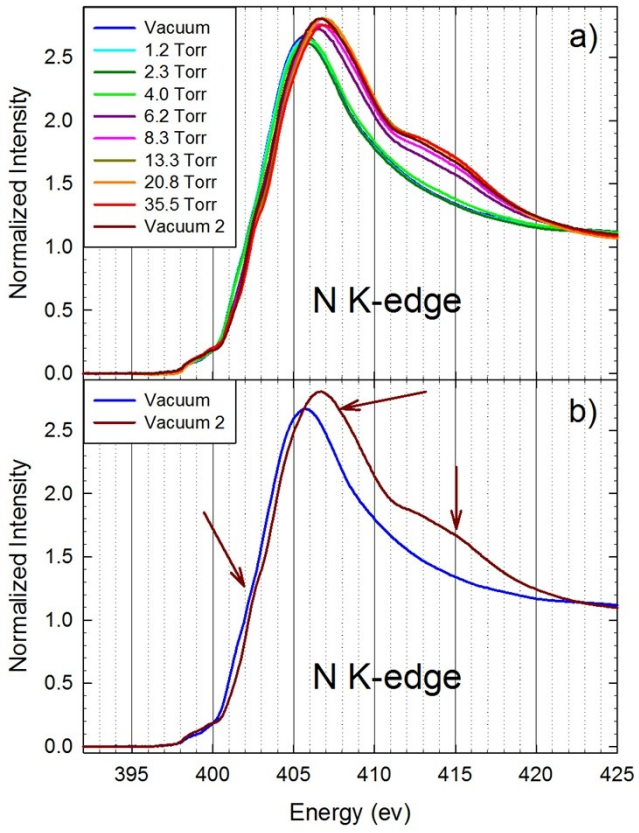

Figure S2: a) Experimental N K-edge spectra of mmen-Mn_2(dobpdc) in vacuum and under increasing pressures of CO_2 gas. Spectral changes do not occur until 6.2 Torr, in accordance with the higher "step pressure" observed for this MOF by McDonald et al. The spectrum does not revert when returning to vacuum, implying that CO_2 remains adsorbed. **b)** Initial and final vacuum spectra only, to make spectral changes clearer. The spectral changes are marked with arrows and are similar to those observed for mmen-Mg_2(dobpdc); namely a new feature near 402 eV (albeit less pronounced than for mmen-Mg_2(dobpdc)), a blueshift in the main edge feature near 405 eV, and a new, broad feature between 411 and 418 eV.

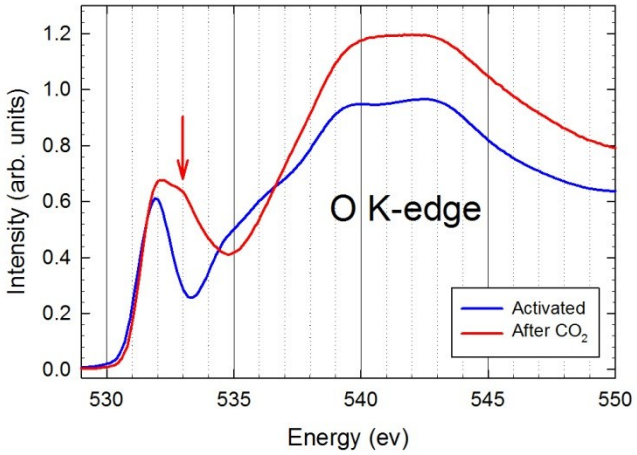

Figure S3: Experimental O K-edge spectra of mmen-Mn_2(dobpdc) before and after CO_2 adsorption. As seen for mmen-Mg_2(dobpdc), a second π^* resonance (marked with a red arrow) appears after adsorption at ~533 eV, approximately 1 eV higher in energy than the first at ~532 eV. The generally increased intensity above the absorption edge reflects the higher optical density of O in the sample after CO_2 adsorption.

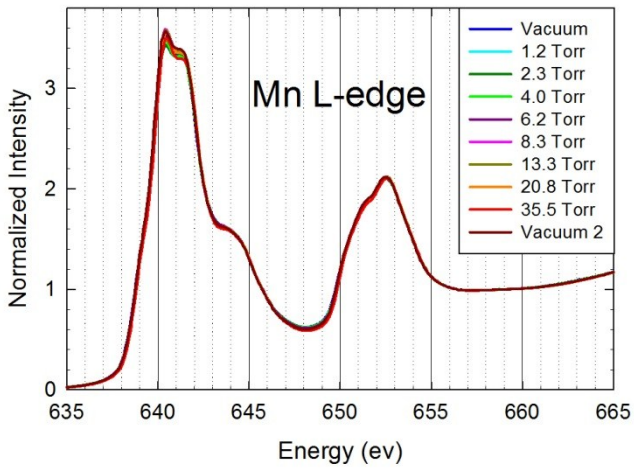

Figure S4: Experimental Mn L-edge spectra for mmen-Mn_2(dobpdc) under vacuum and increasing pressures of CO_2 gas. No spectral changes are observed. The spectra are consistent with a high-spin configuration.

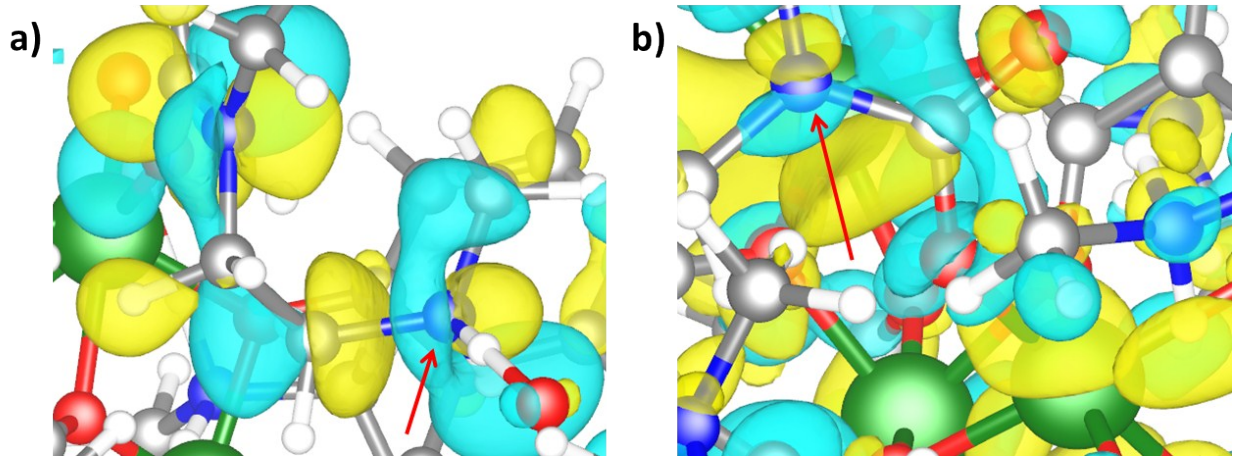

Figure S5: a) Final state wavefunction for a representative transition at 405.2 eV in the computed N K-edge spectrum of the insertion structure. The excited atom is indicated with an arrow. The state shows clear $\boldsymbol{\sigma}^*$ character along the amine chain. **b)** Final state wavefunction of a representative transition between 411 and 419 eV in the computed N K-edge spectrum of mmen-Mg_2(dobpdc). The excited atom is indicated with an arrow. This state is diffuse, extending throughout the unit cell, but shows clear $\boldsymbol{\sigma}^*$ character across the new N-C bond formed upon CO_2 adsorption.

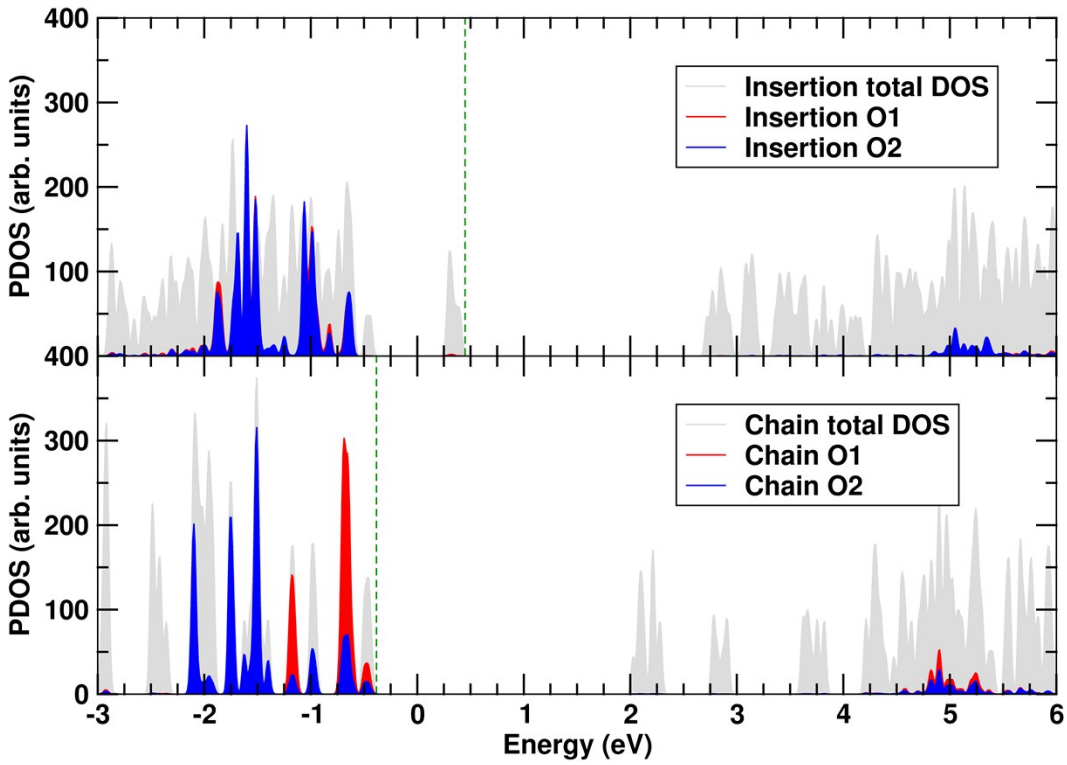

Figure S6: PDOS plots for the insertion structure (top) and chain structure (bottom). The PDOS for the two carbamate O atoms in each structure are shown in red and blue, while the total DOS is shown in grey. The splitting between the occupied and unoccupied states for the carbamate O atoms is nearly identical for each structure (~5.682 eV for the insertion structure and ~5.516 eV for the chain structure).

References:

1. P. Giannozzi, S. Baroni, N. Bonini, M. Calandra, R. Car, C. Cavazzoni, D. Ceresoli, G. L. Chiarotti, M. Cococcioni, I. Dabo, A. Dal Corso, S. de Gironcoli, S. Fabris, G. Fratesi, R. Gebauer, U. Gerstmann, C. Gougoussis, A. Kokalj, M. Lazzeri, L. Martin-Samos, N. Marzari, F. Mauri, R. Mazzarello, S. Paolini, A. Pasquarello, L. Paulatto, C. Sbraccia, S. Scandolo, G. Sclauzero, A. P.

Seitsonen, A. Smogunov, P. Umari and R. M. Wentzcovitch, *Journal of Physics-Condensed Matter*, 2009, **21**.

2. B. Hetenyi, F. De Angelis, P. Giannozzi and R. Car, *Journal of Chemical Physics*, 2004, **120**, 8632-8637.